GeoResJ 14 (2017) 67–79

Contents lists available at ScienceDirect

GeoResJ

journal homepage: www.elsevier.com/locate/georesj

Recent climate warming and the Varas rock glacier activity, Cordillera Oriental, Central Andes of Argentina

Mateo A Martini[a,*], Jorge A Strelin[a,b], Eliseo Flores[c], Ricardo A Astini[a], Michael R Kaplan[d]

[a] Centro de Investigaciones en Ciencias de la Tierra (CONICET-UNC), Vélez Sársfield 1611, X5016GCA Córdoba, Argentina
[b] Instituto Antártico Argentino, Convenio MREC - Universidad Nacional de Córdoba, Vélez Sársfield 1611, X5016GCA Córdoba, Argentina
[c] Facultad de Ciencias Exactas, Físicas y Naturales. Universidad Nacional de Córdoba, Vélez Sársfield 1611, X5016GCA Córdoba, Argentina
[d] Geochemistry, Lamont-Doherty Earth Observatory, Palisades, NY 10964, USA

ARTICLE INFO

Article history:
Received 2 March 2017
Revised 23 July 2017
Accepted 4 August 2017
Available online 9 August 2017

Keywords:
Rock glacier
Protalus lobe
Warming trend
Permafrost
High-altitude
Subtropical Andes
Argentina

ABSTRACT

Recent studies have revealed that in high-altitude mountain environments the global warming trend over the last few decades tends to be strongly amplified. However, few attempts have been made to monitor the possible effects of such climate changes on high-altitude rock glaciers. In this paper, we provide a geomorphic analysis of the Varas rock glacier, and present the first observations of rock glacier temperature (air and ground) and surface velocities in the Andes of northwestern Argentina. A network of 30 boulders was monitored every year between 2012 and 2016 using a differential Global Positioning System. Over the observational period, the Varas active rock glacier registered velocities between 125 and 5 cm/yr, except for four boulders which did not shift. Over the five years of monitoring, the mean annual air and ground (at 5 and 50 cm depth) temperature remained above 0 °C. A long-term instrumental weather dataset (106 years), located ~130 km from the Varas rock glacier, at La Quiaca station, reveals a warming trend of 0.8 °C during the last century, with a steep increase during the last two and half decades. The warming trend recorded in the region may have produced or facilitated the inactivity of the more-exposed sectors of the Varas active rock glacier. However, there also may be a delay in the relatively slow and full response of rock glaciers to the last few decades of warming. Finally, the observations allow us to propose a formation sequence in the Varas rock glacier valley, since postglacial time.

1. Introduction

Rock glaciers are one of the most widespread and common features of the high-altitude cryosphere in the arid to semiarid Central Andes ([1,14,56,58,76] and [4,22,51,59,61]). The recent Argentine National Law protects rock glaciers from impacts produced by mining and industrial activities and therefore their study has acquired great importance in the last few years [71]. Moreover, rock glaciers are potential water resources, vital for agriculture and subsistence of native communities that develop small-scale farming down valley [4,20,51,59,65].

In the tropical and subtropical Andes, warming trends have been reported during the last few decades [24,63,79]. In general, the rate of warming is also amplified with elevation, with greater a rise in high-altitude mountain environments [57]. As a consequence, an increase in elevation of the 0 °C isotherm (freezing level) enlarges the area with positive temperatures, which produces the degradation and restriction of the high-mountain cryosphere (e.g., [17,25,30,78]). For example, during recent decades the glaciated surface area in the tropical and subtropical Andes has been dramatically reduced [39,60]. Hence, the study of the recent glacier wastage has become critical due to the strong dependence of local communities on glacier meltwater for human consumption and agriculture [13]. Yet, the response of the mountain permafrost (e.g., rock glaciers) to regional warming has not been resolved in South America [39,74]. Moreover, general circulation models predict that high-mountain ranges in the low-latitude Andes will be severely affected by temperature rise over the next few decades and centuries [11].

Recently, hundreds of rock glaciers have been reported in northwestern Argentina [2,26,51]. Because of the difficult access, and hard fieldwork conditions above 4500 m a.s.l., most of these rock glaciers have been indentified and inventoried using remote sensing; and their classification into active, inactive or fossils forms has been done using geomorphologic criteria of activity. The activity classification is based on diagnostic features such as: steepening of the front slope, presence of fine material in the front slope, surface structures (ridges and furrows), degree of vegetation cover,

* Corresponding author.
E-mail address: mmartini@unc.edu.ar (M.A. Martini).

http://dx.doi.org/10.1016/j.grj.2017.08.002
2214-2428/

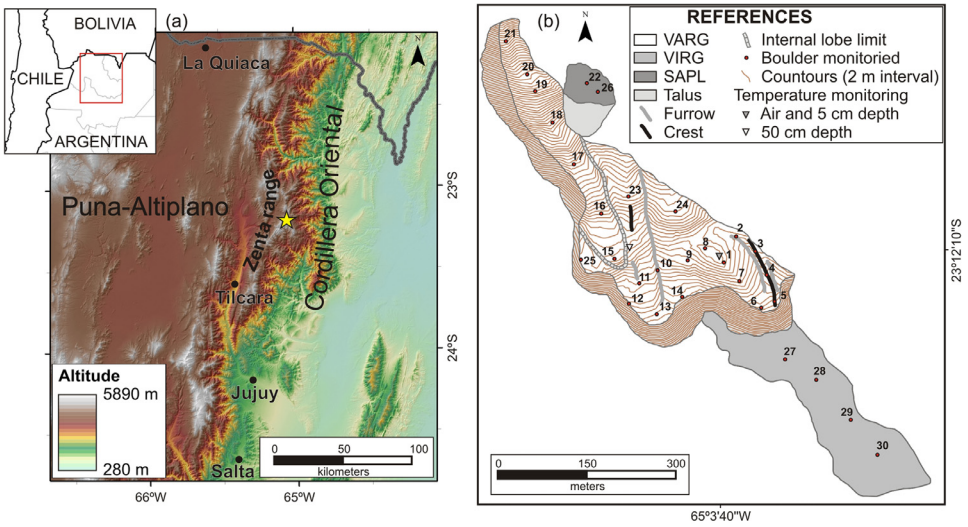

Fig. 1. (a) Digital Elevation Model (based on Shuttle Radar Topography Mission) of northwestern Argentina showing the location of Varas rock glacier (yellow star). (b) Varas rock glacier map with the main geomorphologic features, boulders monitored and temperature data logger location. VARG: Varas active rock glacier; VIRG: Varas inactive rock glacier; SAPL: small active protalus lobe. (For interpretation of the references to color in this figure legend, the reader is referred to the web version of this article).

relationships with the source area, among others [6,16,80]. Such geomorphologic criteria are easily applied and useful to classify rock glacier activity from satellite images, aerial photographs and digital elevation models.

However, obtaining the more difficult measurements of movement and monitoring of temperature are essential, in order to characterize rock glaciers and corroborate the activity criteria used for regional rock glacier inventories based on remote sensing approaches. Flow velocities of rock glaciers have been reported in several places around the world (see [5,45]), but in the Central Andes such measurements are scarce [9,23,41]. Given the small number of South American (and world-wide) high-altitude (>4000 m a.s.l.) meteorological stations, climatic monitoring on active rock glaciers can be used for model validation and detection of changes in regions of the world that are warming the fastes [11,57,77].

In this paper, we provide a geomorphic analysis of the Varas rock glacier (*cf.* [51]), and present the first observations of rock glacier temperature (air and ground) and surface velocities in the Andes of northwestern Argentina. To establish climate trends for the last 106 years, we use and discuss the only regionally available extensive high-altitude air temperature dataset, in nearby La Quiaca. Finally, we discuss the main surface flow conditions, thermal characteristics, and formation of the Varas rock glacier, as well as inferred changes in its dynamics as a result of recent climate change.

2. Regional setting

The Cordillera Oriental of northwestern Argentina (~22–26°S) is a north-south trending mountain range along the eastern border of the Puna–Altiplano plateau (Fig. 1a). The rainfall in Cordillera Oriental is related with the activity of the South American Summer Monsoon [83]. Most of the annual rainfall (~75%) is produced during the austral summer [7], in response to the South American Low Level Jet winds that transport the humidity from the Amazon region to northern Argentina [28]. The moisture trajectory creates an orographic effect across the Cordillera Oriental, where the east side receives ~2000 mm/yr of precipitation and the west side, close to the Puna–Altiplano plateau, ~400 mm/yr. Also, the amount of precipitation decreases with altitude and above 3500 m a.s.l. it is less than 500 mm. The current altitude of the 0 °C isotherm is estimated at 4916 m a.s.l. [51]. The low relative humidity and the low-latitude high-altitude location of the Cordillera Oriental produce conditions of high incoming solar radiation received [64].

The Zenta range is one of the highest ranges within the Cordillera Oriental (Fig. 1a) with a maximum altitude of 5116 m a.s.l. It mainly consists of Precambrian, Paleozoic and Mesozoic clastic sedimentary rocks [29]. At present, the range does not contain glaciers, although during the Late Pleistocene valley glaciers occupied the highest parts of the range, above 3900 m a.s.l. [50]. Rock glaciers lay inboard of marginal moraines in glaciated valleys and generally have south and east orientations. In the Zenta range, Martini et al. [51] inventoried a total of 83 rock glaciers, covering an area of 4.34 km^2, which only about 10% of the rock glaciers are active, showing the prevalence of inactive and fossils forms. The lower limit of active rock glaciers in the Cordillera Oriental (22–25°S) is 4500 m a.s.l. [51], which is lower than the 4700 m a.s.l. reported in the Bolivian Western Cordillera (18–22°S) [61]. A glacial chronology obtained at Nevado de Chañi, about 100 km south of Zenta range, reveals that the last glacial advance in the region took place at ~12 ka [49]. Because rock glaciers are located inboard of the deposits left by the last glacial advance, ~12 ka is considered a maximum age for the rock glaciers of Cordillera Oriental [51].

2.1. The varas rock glacier

The Varas rock glacier (23° 12′ 9″ S; 65° 3′46″ W) is located on the eastern slope of the Zenta range (Figs. 1 and 2), along the south wall of a (formerly) glaciated valley. The substrate consists of cretaceous conglomerates and sandstones (Pirgua Subgroup; [29]). Based on the position, it is classified as a talus-derived rock glacier, indicating a periglacial origin [5]. First described by Martini et al. [51], based on morphological characteristics, it was divided into: i) Varas active rock glacier (VARG); ii) Varas inactive rock glacier (VIRG) and; iii) small active protalus lobe (SAPL) (Figs. 1b and 2).

The VARG extends from 4730 m to 4500 m a.s.l., and therefore is situated below the regional 0 °C isotherm (4916 m a.s.l.). It receives debris supply from the valley-wall located immediately above

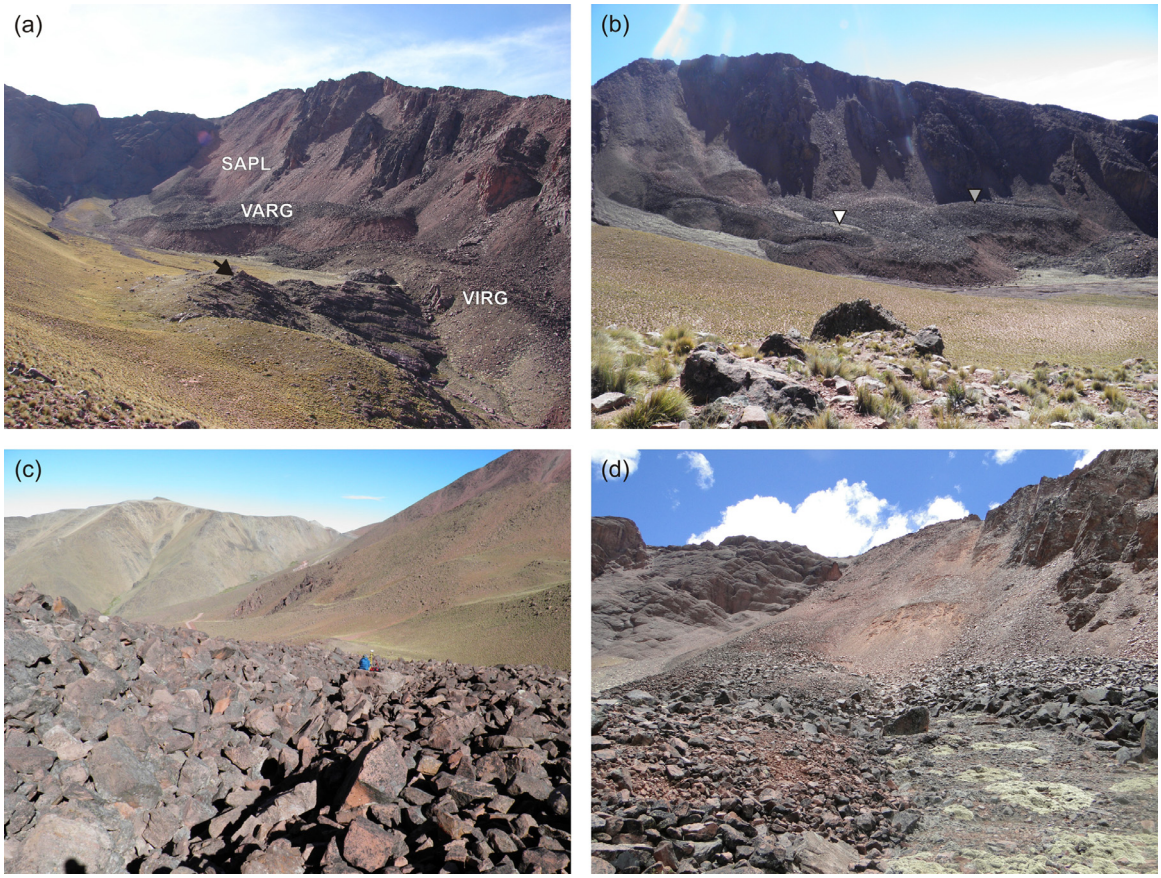

Fig. 2. Field photographs of the Varas rock glacier. (a) Panorama of Varas rock glacier valley (view is looking northwest), showing the VARG, VIRG and the SAPL. The black arrow indicates the striated bedrock where the GPS base station was fixed. (b) Photograph with view looking north towards the VARG and the SAPL. The VIRG is toward the east side of the VARG. The triangles indicate the locations of thermometers: air and ground at 5 cm depth (grey) and ground at 50 cm depth (white). The internal lobe of the VARG is situated immediately ahead of the grey triangle. (c) Photograph of the surface of the VARG. Note the open-work fabric and size of the boulders. (d) Photograph from the VARG with view looking northwest. In the bottom of the photo is the VARG surface with boulder material (left) and fine-sediments with vegetation (green patches on the lower-right corner). The SAPL is in the center back of the photograph. (For interpretation of the references to color in this figure legend, the reader is referred to the web version of this article).

(Fig. 2), where the highest peaks reach 4900 m a.s.l. It has a maximum length of 690 m and a maximum width of 230 m. Most of the VARG surface is situated below the valley-wall, except for a small sector that lies on the valley bottom (Fig. 2). The VARG covers an area of 0.10 km^2 and the mean thickness of its front is ~16 m. Its surface is composed of big boulders, reaching up to 3 m in diameter, with an open-work fabric; hence the feature can be classified as a bouldery rock glacier (cf. [36]) (Fig. 2c). Longitudinal ridges and furrows are present on its surface, and an internal lobe is developed on the upper sector (Figs. 1b and 2b). Only a small bar located immediately to the east of the internal lobe exhibits fine sediments and vegetation (Fig. 2d). The frontal slope has an angle of 35° and is composed of a mixture of boulders and fine sediments. No exposed ice has been recognized in the VARG.

The VIRG has an area of 0.03 km^2 and extends down to 4410 m a.s.l. On its upper part the form has been partially overridden by the active sector (VARG, Fig. 2a). The VIRG has neither ridges nor furrows in its surface. It is composed of boulders covered by lichens, and fine sediments and herbaceous vegetation fill the space between boulders. These characteristics and the low front slope angle (31°) denote its inactivity. About 50 m above the VARG, the SAPL is denoted, which compasses an area of ~0.004 km^2. This small body is situated on the steep valley-wall and exhibits a long front slope (in relation with its area), where rock falls are recurrent (Fig. 2d).

3. Materials and methods

3.1. Surface movement

We used a differential Global Positioning System (GPS) to measure once a year the accurate and precise location and altitude of specific markers across the Varas rock glacier (e.g., [45,46]). The equipment consists of two receivers (antennae) Trimble R4 dual-frequency. One receiver was installed in a stable surface (base station) and the other receiver was used to measure a network of markers (rover stations) over the rock glacier.

The base station was installed on striated bedrock near the bottom of the same valley of the Varas rock glacier (Fig. 2a). We built a small monolith of concrete with a bolt to screw in the base station. This structure prevented the receiver from moving over the duration of measurements and ensured the receiver was situated in the same position every year.

The two receivers acquired data simultaneously using a "Fast-Static" survey. For each marker, survey time varied between 8 and 20 min, depending on the number of satellites available. We used the Trimble Business Center (version 2.50) software to make the differential postprocessing correction. First, we made the postprocess between a permanent GPS station at Tilcara (located ~55 km to southeast, Fig. 1a) and our base station. Then, we made the postprocess between our base station and each rover station.

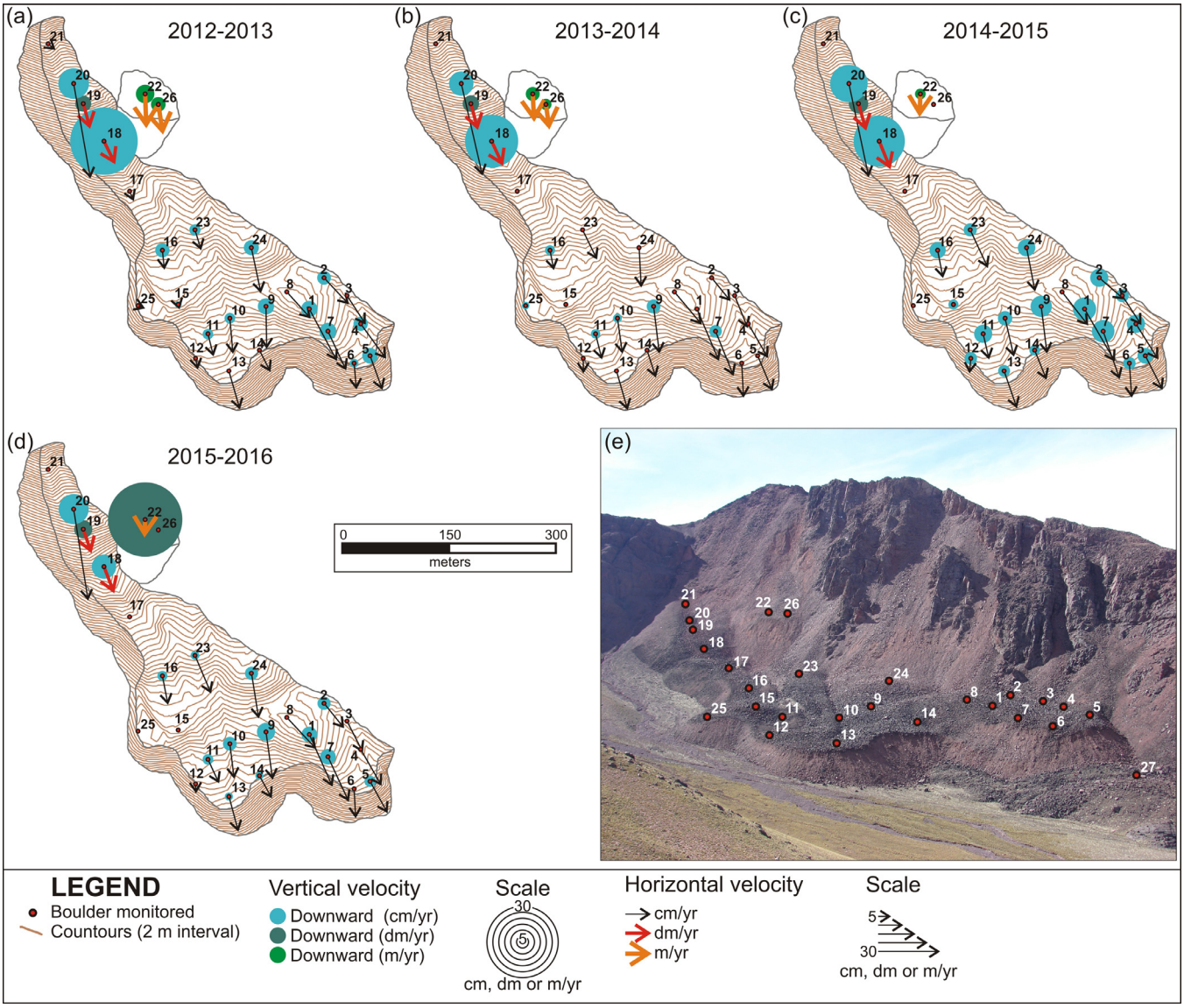

Fig. 3. Varas rock glacier annual surface velocity. Annual vertical (circles) and horizontal (arrows) components of the annual displacement of monitored boulders on the VARG and SAPL during (a) 2012–2013, (b) 2013–2014, (c) 2014–2015 and (d) 2015–2016 periods. Note that circles as well as arrows have different velocity scales (cm, dm or m/yr; as shown in the legend), which is given by their colors, because the velocity values for boulders differ up to two orders of magnitude. (e) View to the north with the approximate position of monitored boulders. On the VIRG only boulder 27 is shown; the rest (boulder 28, 29 and 30) are not in the area shown on the photograph. (For interpretation of the references to color in this figure legend, the reader is referred to the web version of this article).

A survey network of 30 boulders was established as rover stations. Large boulders (diameter between 1 and 4 m) were selected to avoid individual movement of smaller blocks that do not represent rock glacier flow. The distance between rover stations and the base station ranged from 150 to 800 m. To mark each boulder we made a 0.5–1 cm depth hole on its upper surface using a hammer and a drill bit. The rover stations were surveyed by positioning the receiver in top of a rod 1.1 m high, held with a bipod. The rod was positioned vertically using a bubble air level in each boulder mark. Twenty-six of the survey markers are on the VARG, four on the VIRG and two on the SAPL (Fig. 3). The surveys were carried out in April 2012, 2013, 2014, May 2015 and April 2016. Comparing the position of each rover station between consecutive years, we calculated the horizontal and vertical displacements, and their resulting vector (including deep and direction angles) of the 30 survey markers. We assumed no vertical or horizontal movement of a boulder when the displacement measured was $\leq 2\sigma$ error propagation. The uncertainty associated with the displacement vectors was calculated using the weighted 1σ error of each variable [72] from:

$$\sigma v = X * \frac{\sigma x}{V} + Y * \frac{\sigma y}{V}$$

where σx, σy and σv are the horizontal, vertical and vector 1σ error, respectively; and X, Y and V are the horizontal, vertical and vector displacement, respectively. In order to generate a surface velocity map of the VARG we interpolated boulder velocities using the Kriging method.

To map the topography of the VARG, we walked throughout its surface with the rover station and measured points every 5 s (time interval) using a "kinematic" survey. A total of 3479 points were surveyed, from which the topography of the VARG was generated (Fig. 1b).

3.2. Temperature monitoring

Three temperature data loggers were installed on the VARG (Figs. 1b and 2b). Two of them were installed at 4566 m a.s.l, between boulders with open fabric: one for air temperature at 150 cm above the rock glacier surface (which includes a radiation shield), and the second for ground temperature at 5 cm below the surface. The third data logger was installed ~150 m west of the other two, at 4588 m a.s.l., and it was buried at 50 cm depth in a small zone with fine sediments (gravel size and smaller) (Fig. 1b).

The temperature data loggers consist of Ondotori model TR-52 thermometers (resolution 0.1 °C; accuracy 0.3 °C), and were configured with an hourly measurement interval. The periods of time recorded were from 9 April 2010 to 21 April 2016 (air and 5 cm depth) and from 11 October 2010 to 21 April 2016 (50 cm depth). There are no gaps in data coverage during the time recorded. To estimate the snow cover duration over the VARG we analyzed the ground temperature at 5 cm depth. Snow cover was considered when the ground temperature amplitude was ≤1 °C and the temperature ranged between +1.5 and −1.5 °C.

3.3. Long-term analysis of temperature from la quiaca station

Above 3000 m a.s.l. climate instrumental series in the Central Andes of Argentina are limited. An exception, the La Quiaca station at 3459 m a.s.l., has a long-term temperature record since 1911 and represents the most extensive and continuous record in the high altitudes of Argentina. This record is situated ~130 km northwest of the Varas rock glacier in a similar high-altitude relatively arid geographical setting (Fig. 1a). The relative proximity and similar setting make it an ideal site, to compare with our short-term temperature record from the Varas rock glacier.

Two monthly air temperature series from La Quiaca were analyzed: i) “series 1” from the Global Historical Climatology Network (<climexp.knmi.nl/>); ii) “series 2” from Argentina’s Servicio Meteorológico Nacional (personal communication). We selected series 1 as our base series because it extends to the present. The missing data of series 1 was partially filled in using data of series 2. The missing data which could not be filled using series 2 (1.6% of the total), was then obtained by calculating an average for the 10 years before and 10 years after each missing data point. The final series encompasses 106 years of record from 1911 to 2016. The series was not compared with any other because the available records comprising similar periods of time are distant and located in the lowlands, where the geographical and climatic settings are different (warmer and wetter climate; e.g., Jujuy or Salta stations).

To evaluate the correlation between the monthly temperatures of La Quiaca and at the Varas rock glacier, we made a linear regression and calculated the Pearson coefficient (R). To assess the annual temperature trends at La Quiaca from 1911 to 2016, we employed the Mann–Kendall test [44,48]. The Kendall coefficient (τ) was estimated in order to evaluate if the trend is positive or negative, whereas the p parameter was used to assess if the trend is statistically significant. Assuming the temperature variation in time is linear; we estimated the line slope using Sen’s parameter [66]. In order to examine monthly temperature trends we used the seasonal Kendall test [35].

4. Results

4.1. Surface movement

Annual surface displacements of each monitored boulder are shown in Figs. 3 and 4, Table 1 and the Supplementary material. The measured points contain a horizontal ± 1σ error that ranges from 0.2 to 0.9 cm, with an average of 0.4 cm. Vertical ±1σ error ranges from 0.4 to 1.9 cm, with an average of 0.8 cm. The average surface velocity on the VARG for the entire period (2012–2016) is 22.2 cm/yr. The 2014–2015 period presents the highest average (24.2 cm/yr), followed by the 2015–2016 period with 22.2 cm/yr. The 2012–2013 and 2013–2014 periods have the same average surface velocity within error (21.7 cm/yr).

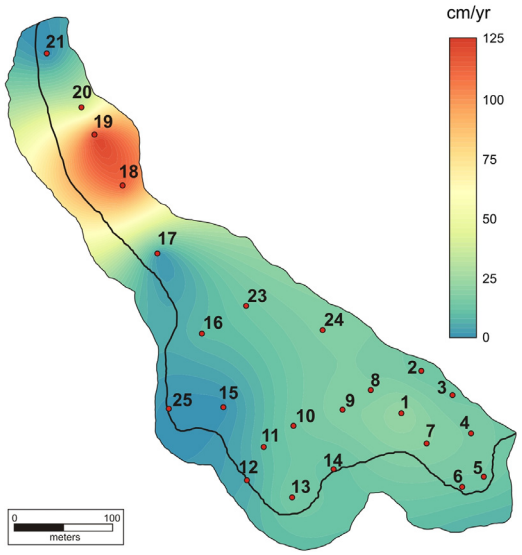

Fig. 4. Mean surface velocity of the entire VARG during the 2012–2016 period, estimated from interpolation of the 24 measured boulders (numbered). Note that the highest rates are near the top (boulders 18–20), the lowest rates are around the lower left and right sides, and no-movement is recorded on boulders 15, 17, 21 and 25. The dark line on the VARG indicates the slope limit. Data used are in Table 1.

The boulder movements on the VARG exhibit a high spatial variation, although distinct patterns are observed. Four boulders (15, 17, 21 and 25) had no movement during the 2012–2016 period. Displacement on boulders 17 and 21 was only detected during the 2012–2013 period (4.0±0.9 and 3.5±0.8 cm, respectively). Boulder 15 exhibited displacement during the 2012–2013 period (2.8 ± 1.1 cm) and the 2014–2015 period (3.6 ± 1.7 cm), but in the later period only in the vertical. Boulder 25 had 2.7 ± 0.6 cm of displacement over 2012–2013 and 2.6 ± 0.6 cm over 2013–2014. Nevertheless, during the later period boulders had a west direction of movement (286°), that is, opposite to the movement direction (112°) over the 2012–2013 period, and very different to the mean direction (161°) of the rest of the boulders in the VARG. In all the cases of boulders 15, 17, 21 and 25, it is not possible to detect movement when we compare the first and the last year of measurement (2012–2016 period). Therefore, we consider the small movements of these boulders, just recorded in some years, as shifting of the blocks, which does not represent the rock glacier flow.

The other 20 boulders of the VARG reveal surface displacement. The mean velocity for the 2012–2016 period ranges from 4.9 ± 0.7 cm/yr (boulder 12) to 124.9 ± 1.2 cm/yr (boulder 19). Disregarding the boulders with no-movement (15, 17, 21 and 25) we can divide the VARG into: i) an upper zone, where the velocity ranged between 40 and 125 cm/yr (boulders 18, 19 and 20), and ii) a lower zone, where the velocity ranged between 5 and 24 cm/yr (boulders 1–14, 16, 23 and 24). These two zones are separated by boulder 17. Boulders 18 and 19 exhibited the largest velocities of the VARG (111.5 ± 1.0 and 124.9 ± 1.2 cm/yr, respectively), between 3 and 23 times higher than the rest. The horizontal movement of the VARG showed similar behavior during different years. In turn, the vertical movement exhibited different magnitudes through the years (Fig. 3). For example, during the 2013–2014 period, 16 of a

Table 1
Surface velocity of each point monitored from individual years and during the entire period of measurements (four years). Deep and direction (strike) are the vertical and horizontal angles of the vector movement, respectively. They are calculated for the entire period 2012–2016. The surface slope is shown only for the VARG.

Boulder	Velocity $\pm 1\sigma$ (cm/yr)					Angle (°)		Surface slope (°)
	2012–2013	2013–2014	2014–2015	2015–2016	2012–2016	Deep	Direction	Deep
1	24.5 ± 1.0	22.8 ± 0.7	26.1 ± 1.3	23.7 ± 1.0	24.2 ± 0.9	14	154	8
2	15.6 ± 1.7	11.9 ± 1.5	15.0 ± 2.4	13.6 ± 1.4	13.9 ± 1.1	20	138	14
3	13.8 ± 0.8	14.0 ± 1.2	14.9 ± 1.7	14.1 ± 0.9	14.0 ± 0.6	0	151	17
4	18.2 ± 1.2	15.8 ± 0.9	18.4 ± 1.4	16.8 ± 0.7	17.3 ± 0.8	15	148	14
5	15.7 ± 1.8	15.2 ± 1.0	16.3 ± 1.2	15.2 ± 1.0	15.5 ± 1.3	17	155	15
6	10.8 ± 1.1	13.7 ± 0.7	14.6 ± 0.7	11.6 ± 0.4	12.7 ± 0.7	13	177	14
7	18.5 ± 1.1	19.9 ± 0.8	22.2 ± 1.0	20.8 ± 0.9	20.3 ± 0.9	19	158	17
8	14.2 ± 0.5	17.0 ± 0.6	17.0 ± 0.7	17.3 ± 0.7	16.4 ± 0.5	0	139	11
9	18.2 ± 0.8	19.9 ± 0.9	21.0 ± 1.1	20.7 ± 1.0	19.9 ± 0.9	20	174	15
10	14.9 ± 0.9	14.6 ± 1.0	16.8 ± 1.2	14.9 ± 1.0	15.3 ± 0.9	17	171	19
11	10.0 ± 1.1	10.9 ± 0.9	12.4 ± 1.3	11.1 ± 1.1	11.0 ± 1.2	24	164	15
12	4.3 ± 0.6	5.9 ± 0.5	7.6 ± 1.3	3.5 ± 0.6	4.9 ± 0.7	0	179	15
13	15.9 ± 0.5	16.3 ± 0.5	16.3 ± 0.9	14.8 ± 0.8	15.8 ± 0.8	9	163	15
14	9.7 ± 0.7	11.5 ± 0.5	13.4 ± 0.8	10.7 ± 0.9	11.4 ± 1.1	13	156	11
15	2.8 ± 1.1	0	3.6 ± 1.7	0	0	–	–	14
16	9.3 ± 1.1	8.6 ± 1.2	12.7 ± 1.7	12.3 ± 1.3	10.7 ± 1.3	26	170	14
17	4.0 ± 0.9	0	0	0	0	–	–	21
18	104.2 ± 0.9	108.9 ± 0.8	121.3 ± 0.8	112.8 ± 0.8	111.5 ± 1.0	10	157	25
19	120.4 ± 1.8	123.8 ± 2.5	133.4 ± 2.0	122.5 ± 1.4	124.9 ± 1.2	33	164	29
20	40.9 ± 1.2	39.4 ± 1.9	41.6 ± 2.1	39.3 ± 1.3	40.3 ± 1.2	18	169	12
21	3.5 ± 0.8	0	0	0	0	–	–	24
22	1524.3 ± 2.0	1205.7 ± 2.1	966.9 ± 1.4	745.0 ± 1.3	1109.9 ± 1.2	26	182	
23	9.3 ± 1.0	13.2 ± 0.6	17.6 ± 1.0	16.9 ± 0.9	14.2 ± 1.1	14	157	14
24	19.3 ± 0.9	15.9 ± 0.6	19.1 ± 1.0	19.0 ± 0.8	18.3 ± 0.8	15	171	10
25	2.7 ± 0.6	2.6 ± 0.6	0	0	0	–	–	10
26	1314.0 ± 2.3	1060.5 ± 2.2	n/d	n/d	1187.0 ± 1.3[a]	24[a]	171[a]	
27	2.3 ± 0.5	3.2 ± 1.4	0	0	0	–	–	
28	0	0	0	0	0	–	–	
29	0	0	0	0	0	–	–	
30	0	1.3 ± 0.5	0	0	0	–	–	

[a] Boulder 26 was not found during the 2015 survey and in the following years. The 2012–2014 period is used to calculate its mean annual velocity.

total of 24 boulders did not present vertical movement. The vertical movement (when detected) was always downward. For the boulders that exhibited movement throughout the entire period, only for three (4, 8 and 12) was the displacement exclusively horizontal. For the rest, the horizontal movement was between 2 and 6 times greater than the vertical movement.

In the VIRG, no movement was detected during the entire period (2012–2016). It was possible to detect small movements in some years for boulders 27 and 30 (Table 1). During the 2012–2013 period, boulder 27 had a horizontal displacement of 2.3 ± 0.5 cm, but with 347° direction, which is opposite to general slope and the VARG movement. Similarly, during the 2013–2014 period boulder 30 had a horizontal displacement of 1.3 ± 0.5 cm with 23° direction. We interpret the movement detected in boulders 27 and 30 as a consequence of sample shifting that is not related with possible flow of the VIRG.

The SAPL had an extremely high annual velocity. During the 2015 and 2016 surveys, we did not find the boulder 26. Boulders 22 and 26 had a mean annual displacement of 11.1 and 11.9 m, respectively (the latter only for the period 2012–2014). Due to the high velocity and its position near the front, boulder 26 probably fell down the slope and therefore was not found during 2015 and 2016 surveys. Boulder 22 reduced its displacement by a rate of ~20% every year. During the 2012–2013 period, boulder 22 was displacement 15.2 m, decreasing to 7.4 m during the 2015–2016 period. Between 2012 and 2016, boulder 22 had a vertical displacement of 19.4 m.

4.2. Temperature record

The three thermometers installed in the VARG exhibited positive mean annual temperatures between 2011 and 2015 (Fig. 5 and Table 2). Ground temperature at 5 cm depth in coarse material was higher than that at 50 cm depth in fine sediments, and air temperature was lower than both 5 and 50 cm ground temperatures. A comparison between the air and 5 cm depth records, during measured years, indicates that 2011 and 2013 had a similar mean annual temperature and were colder than in 2012 and 2014. The warmest year of the recorded is 2015.

Most of the mean monthly temperatures were above 0 °C including several winter months (Fig. 5). The thawing index is between 12 and 24 times greater than the freezing index for air temperature (Table 3). The number of days in a year when the temperature did not exceed 0 °C was ≤7 for air and at 5 cm depth, but this increased to 18–36 at 50 cm depth (Table 2). Ground (at 5 and 50 cm depth) daily temperature exhibited a higher variation during the warmer and wetter months (summer) than during the colder and drier months (winter). The high daily temperature amplitude at 5 cm depth was reflected in the abundant freezing-thawing daily cycles recorded (Table 3). At 50 cm depth the daily temperature amplitude was <3 °C during the summer, and <0.5 °C during the winter, indicating that the maximum and minimum temperature are close together at this position under the surface.

Over a total of eight field seasons, carried out either during the end of the dry season (October) or the end of the wet season (April), we did not find snow in the rock glacier or in the surrounding area (Fig. 2). The historical (106 years) mean annual precipitation of La Quiaca is 329±88 mm. During the years covered by our temperature record at the VARG (2010–2015), the annual precipitation values range within $\pm 1\sigma$ of the historical mean, except for the year 2013 when it was 122 mm higher. Using the 5 cm depth ground temperature at the VARG, we identified a total of 42 episodes of snow accumulation (Table 3). Thirty-four of them occurred between November and March (i.e. during the warm and wet season). Although the year 2013 was wetter than the histor-

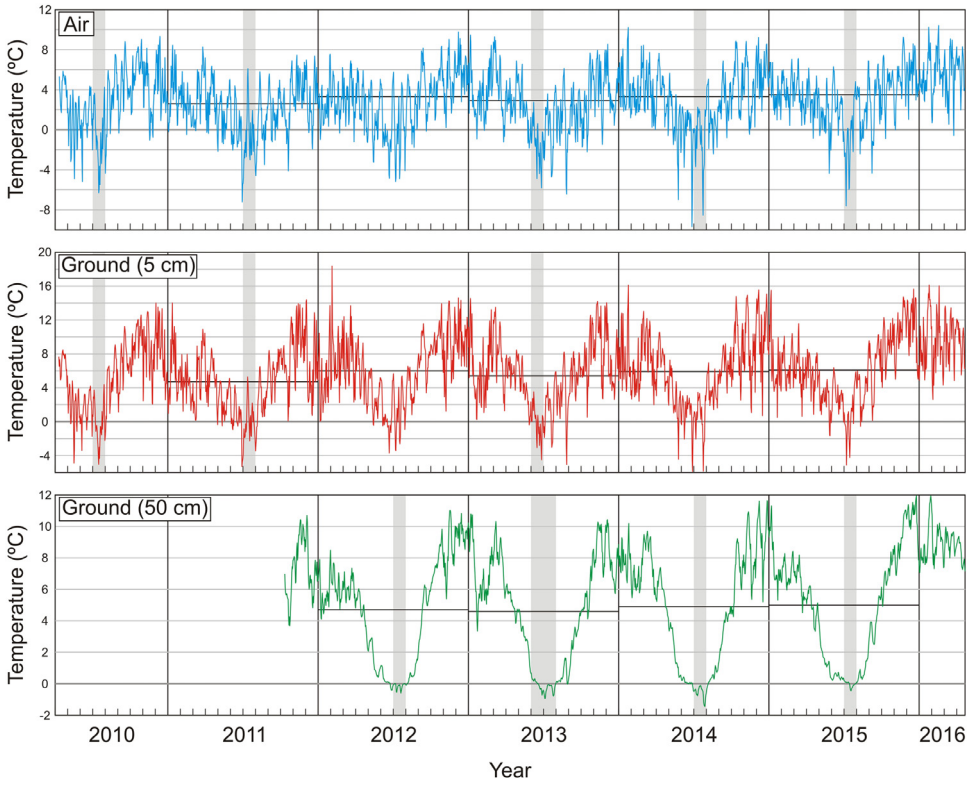

Fig. 5. Varas rock glacier temperature record. Mean daily temperature is shown, which is calculated based on hourly data of air (top), ground at 5 cm depth (middle) and ground at 50 cm depth (bottom). See Figs. 1 and 2B for locations of the thermometers on the VARG. Vertical grey bars indicated the months with mean temperature bellow 0 °C. Horizontal black lines denote the mean annual temperature. Note that the *Y*-axes scale changes between the three plots.

Table 2
Annual temperature characteristics. Thermometer at 50 cm depth started to register in October 2011, so values are shown starting in 2012.

	Mean (°C)					Days with maximum temperature <0 °C					Mean daily amplitude				
Thermometer	2011	2012	2013	2014	2015	2011	2012	2013	2014	2015	2011	2012	2013	2014	2015
Air (+1,5 m)	2.6	3.3	2.9	3.3	3.5	5	2	7	5	5	6.9	7.1	7.2	7.3	7.3
Ground (−5 cm)	4.7	6.0	5.4	5.9	6.1	3	0	0	1	0	13.0	17.3	16.8	17.4	19.5
Ground (−50 cm)	–	4.7	4.6	4.9	5.0	–	18	35	36	15	–	0.8	0.7	0.8	0.8

Table 3
Number of snow cover episodes and freeze-thaw cycles based on 5 cm depth ground temperature.

	2010[a]	2011	2012	2013	2014	2015	2016[b]
Snow cover episodes	0	18	4	6	6	7	1
Freezing-thawing cycles	169	148	143	173	162	174	11

[a] Counting starts on 9 April.
[b] Counted until 20 April

ical mean, the snow cover episodes did not increase during this year (Table 3). Periods of snow cover on the VARG had a short duration with an average of 17 h. Some of these snow accumulation episodes were possible to check using daily satellite Terra MODIS images. In other cases snow cover was not possible to confirm due to cloud coverage in the satellite images or because of the short time of snow occurrence. The longest period when the VARG was covered by snow lasted 88 h. During this time the air temperature showed hourly variations, whereas the 5 cm depth temperature kept close to 0 °C with no variation (Fig. 6).

4.3. La quiaca long-term temperature trend

The monthly mean air temperature record from La Quiaca station and the Varas rock glacier exhibit a significant ($p<0.0001$) highly linear correlation ($R = 0.88$). This allows us to evaluate the long-term monthly temperature record from La Quiaca to assess the high-altitude air temperature trend in the region, including at the Varas rock glacier.

La Quiaca station experienced a positive statistically significant ($p < 0.001$) mean annual air temperature trend during the 1911–2016 period ($\tau = 4.35$). The Sen's slope is 0.008, representing a temperature increase of 0.8 °C from 1911 to 2016. The months that presented the highest seasonal Kendall trends are June, July and August (4.0, 3.8 and 3.7; respectively). In turn, February, March and April did not show any significant tendency ($p > 0.05$) (Table 4). Since 1991, the mean annual air temperature anomaly was positive, except for 2008 when it was negative (Fig. 7). The mean annual temperature prior to 1991 is 9.3 °C and the mean annual tempera-

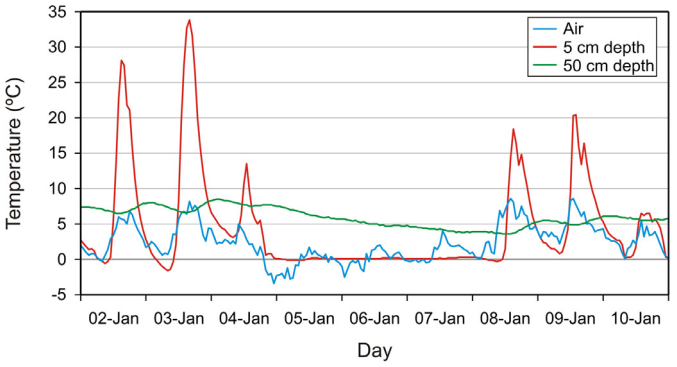

Fig. 6. Temperature during the longest period (88 h) of snow accumulation observed on the VARG. This occurred from 5 to 8 January 2012. Note that during the 88-h episode of snow cover, the ground temperature (green and red) does not show considerable variation, which is contrary to the air temperature (blue). (For interpretation of the references to color in this figure legend, the reader is referred to the web version of this article).

Table 4
Seasonal Kendall test results and p parameter for the La Quiaca dataset (1911–2015). The highest monthly temperature trends are from June, July and August.

Month	Seasonal Kendall test	p
January	1.9	0.0264
February	0.4	0.3356*
March	1.3	0.0946*
April	1.5	0.0718*
May	3	0.0016
June	4	0
July	3.8	0.0001
August	3.7	0.0001
September	2.3	0.0099
October	3	0.0013
November	1.8	0.0378
December	2	0.0217

* Not statistically significant ($p > 0.05$).

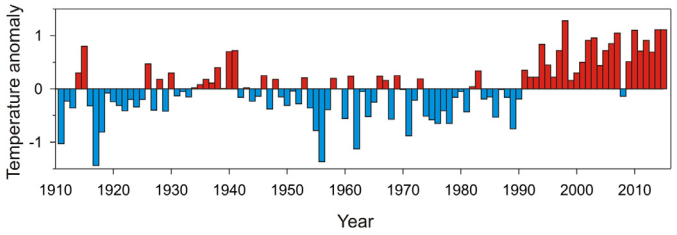

Fig. 7. Annual temperature anomalies at the La Quiaca station from 1911 to 2015. Note that from 1991 to 2015 the annual anomaly was always positive, except during 2008.

ture post-1990 is 10.2 °C, with an abrupt warming of 0.9 °C during the last two and half decades.

5. Discussion

5.1. Ground thermal condition

The temperature record shown in Figs. 5–7, provides insights into the processes affecting the Varas Rock glacier, and other rock glacier landforms in the arid subtropical Andes. Snow can impact rock glacier behavior because it is generally a poor heat conductor, thus, a thick snow cover on the surface insulates the ground beneath from the atmospheric temperature variations [40]. This condition has been recorded farther south in the Central Andes of Chile at 33.5°S [3,10], when an early winter snow-cover insulates the ground from surface temperature, which remains until the beginning of the spring. In the case of latitudes around 33–34°S, however, the snow precipitation is related to the westerly wind activity, which occurs mainly during the winter.

In contrast, in the more northerly Cordillera Oriental the precipitation season occurs during the summer months and is related with the activity of the South American Summer Monsoon. The presence of temperatures well above 0 °C on the VARG during the wetter season rapidly removes the snow on the ground. For instance, during the day prior to the onset of snowfall shown in Fig. 6 (maximum snow cover recorded), the maximum ground temperature at 5 cm depth reached 13.5 °C, and the day when the snow disappeared the maximum temperature was 18.4 °C. Under this relatively high-temperature situation, the snow is rapidly removed and the ground temperature (at least at 5 and 50 cm depth) is coupled to air temperature variation and, hence, is affected by atmospheric changes all year round (Fig. 5). The absence of persistent snow cover on the VARG, including winter, facilitates a low albedo, which increment the amount of energy received from the intense incoming solar radiation and, consequently, affects the ground temperature. Furthermore, due to the open work fabric and the absence of snow cover, in most of the area of the VARG (Fig. 2c) the air can move easily into and throughout the framework of boulders, with such movement controlled by temperature contrasts (convection) [33]. The ground temperature results at 50 cm depth are well above 0 °C over the entire duration of record (Fig. 5) indicating that the active layer extends even deeper.

5.2. Surface flow condition

The highest flow velocities (horizontal and vertical) in the VARG are located in the upper zone (area of boulders 18–20), with the exception of the highest elevation boulder 21. The rates of displacement of boulders 18 and 19 (112 and 125 cm/yr, respectively), which are between 3 and 23 times higher than the rest, coincides with the highest surface slopes of the VARG (Figs. 3 and 4, Table 1). In this sector, the debris supply must be higher and probably the ice supply too, whether from melting and subsequent refreezing at depth, or from sporadic snowbanks that are covered with debris that protect them from melting, with the subsequent formation of ice lenses. In general, high surface velocities on small rock glaciers located on marginal periglacial environments have been attributed to ice thermal conditions close to the melting point (e.g., [37,38,67]). The positive mean annual ground and air temperature (Fig. 4), as discusses above, combined with the steep surface gradient and a higher ice/detritus relation, could generate the high surface velocities in the upper zone of the VARG. Because of the absence of movement registered in boulder 21, it is possible that it corresponds to the lower part of the talus, i.e., the rooting zone of the VARG. In turn, the inactivity of boulder 17 is difficult to explain. Since this boulder is situated in the internal lobe of the VARG a surface velocity intermediate between boulders 18 (~112 cm/yr) and 16 (~11 cm/yr) would be expected.

In the lower zone of the VARG, the surface movement decrees (Fig. 4). In this zone, the lowest velocities and even records of no movement are located near the valley bottom (e.g., boulders 11, 12, 15, 16 and 25), where the surface gradient is reduced and the exposure to incoming solar radiation is higher. On the other hand, the sector of the VARG near the valley-wall (south face) is more protected from incoming solar radiation and shows higher surface velocities (e.g., boulders 1, 7, 9 and 24) (Figs. 2 and 3). The different settings of exposure to solar radiation over these two sectors of the lower part of the VARG could generate different thermal regimens, with higher subsurface temperatures in the more exposed sectors and, consequently, a thicker active layer and less ice/detritus

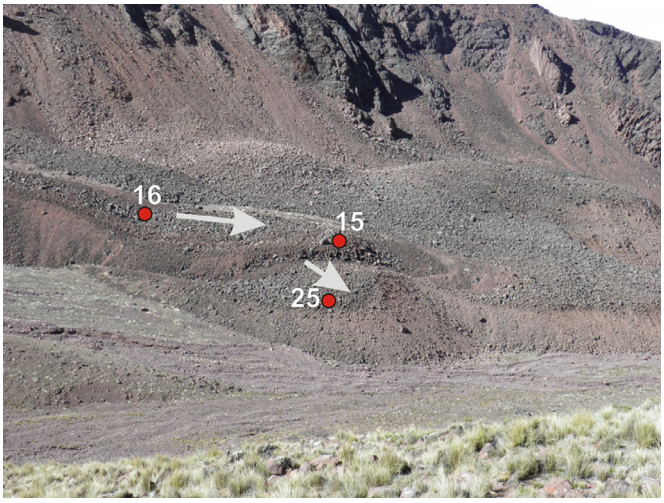

Fig. 8. Photograph of the area of contact between the internal lobe and the setting of boulder 25 in the VARG. Red dots and numbers indicates the approximately positions of the boulders monitored. Arrows show the flow direction of the internal lobe and the inferred flow direction of the boulder 25 area before it turned inactive. Note the difference in the angle and color for the slope near boulder 25, compared with the slope shown all the way on the right side of the photograph. (For interpretation of the references to color in this figure legend, the reader is referred to the web version of this article).

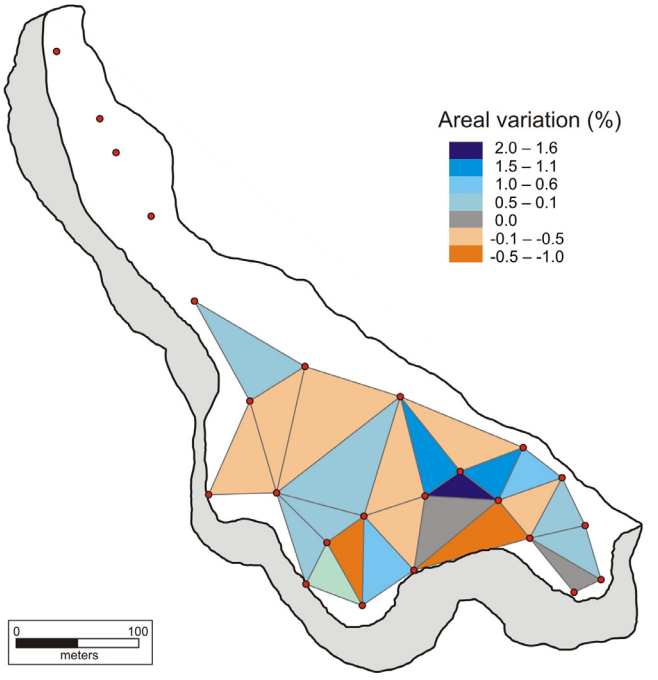

Fig. 9. Areal changes between 2012 and 2016 for the 23 triangles constructed in the lower sector of the VARG. The grey area represents the talus slope.

relation. Therefore, the contrasting surface activities in the lower parts of the VARG could be attributed to unequal exposure, of the two above mentioned sectors. Differences in the incoming solar radiation amount, due to diverse topographic conditions, have been demonstrated to be quite impactful on the rock glaciers distributed along the Central Andes [4,10,15,51,65]. As was noted, the lack of snow cover over long time periods would also significantly increment the solar radiation incidence on the VARG energy fluxes.

To elucidate further the inactivity near boulder 25, we propose another explanation that could be complementary to that mentioned above. Around boulder 25 the rocks exhibit a dark weathering surface indicating a protracted time of exposure and hence relative stability (Fig. 8). This is in agreement with our surface movement results that show no movement for boulder 25. The inactivity of boulder 25 and its surrounding area could be related with the formation of the internal lobe of the VARG that includes boulders 15 to 21 (Figs. 1b and 2b). This internal lobe has an average flow direction of 163° while the boulder 25 area, due its shape and position, should have a southerly flow direction (Figs. 8 and 2b). The internal lobe formation could have changed the flow direction in the sector immediately upward the boulder 25, and cut off the previous flow towards the area of boulder 25. This could have generated a break of debris supply into the area of boulder 25, additionally contributing to it turning inactive.

To help evaluate further areal changes in the lower sector of the VARG, we used the monitored boulder distribution to construct a net of triangles, using each boulder as vertex (e.g., [46]). Comparing the changes in triangle areas during the monitoring period allows the identification of either compressing or extending flow. Fig. 9 shows the distribution of the 23 constructed triangles and the relative areal change between 2012 and 2016. A total of 12 triangles were reduced in area, 2 remain with the same area, and 9 of them increased in area. Compressing and extending flow are associated with negative and positive areal changes; respectively (Fig. 9). The triangle area variation across the VARG displays a complex distribution with no clear pattern. The total area that compasses all the triangles has increased by 25 m^2. This behavior is typical of rock glacier flow generally experiencing extension. An interpretation of an area of net extension is supported by the lack of transverse geomorphic features (e.g., crests) in the lower sector of the VARG (Fig. 1b). Moreover, most of the boulders that exhibit vertical displacement show that the vector angle is greater than the rock glacier surface slope (Table 1). This means a lowering of the surface has occurred in the VARG that could be interpreted as a consequence of extending flow, or because a loss of interior ice lenses in response to melting. Both processes can occur simultaneously. The VARG does not show signs of ice lose on its surface, such as evident by thermokarst or depressions, which could be explained by a low internal ice concentration due to the low-precipitation regime in the arid Cordillera Oriental.

No movement was recorded in the VIRG indicating the absence of flow, except for small displacements in boulders 27 and 30, which are interpreted as boulder shifts possibly associated with thawing and freezing of the active layer or permafrost degradation at depth. The inactivity of the VIRG during four consecutive years is consistent with its classification based on geomorphologic interpretations. The upper limit of the VIRG (4500 m a.s.l.) also coincides with the regional lower limit of active rock glaciers for the Cordillera Oriental [51].

The high velocity of the SAPL (~12 m/yr) exceeds by a fair amount the velocity of the VARG and rock glaciers in general [5]. The relatively rapid flow denotes that the SAPL is a feature under formation on the steep wall immediately above the VARG (Fig. 2). During fieldwork, rock falls and small debris flows from immediately above the SAPL that ended on its surface, were usually observed. The high velocity of the SAPL cannot be explained by internal deformation alone. Other processes, such as basal sliding between the rock glacier and the bedrock [34] have been proposed to explain high displacement rates on rock glaciers. Boulder 22 has a decelerated by 20% per year, which could be attributed to a gradient change (from a higher gradient sector to a less steep gradient near the front slope). Based on the high velocity and the small area of the SAPL, we infer the boulder 22 will soon reach the frontal edge of the SAPL and it will fall onto the front slope, similar to what we interpreted for boulder 26 that was not found after the 2014 field survey.

A comparison of boulder velocities with the local Varas rock glacier temperature record, along the limited time interval considered in our study (2012–2015), does not allow us to find a clear correlation between these parameters. We conclude that we need a more protracted track or length of time in order to attempt a meaningful comparison. Based on numerical models and direct observation (e.g., air temperature and surface velocity) Kääb et al. [43] found that air temperature changes can affect rock glaciers velocities, especially when the permafrost temperature is close to 0 °C. For instance, a warming stage could trigger the occurrence of liquid water in the rock glacier body producing high spatial (as found in the VARG) and temporal variability in the surface movement of rock glaciers. More data, including a longer time record of movement and climatic monitoring, and internal structure surveys are needed in order to evaluate the mechanisms responsible for the VARG surface dynamics.

5.3. Climate change and the Varas rock glacier

By comparing the temperature record on the Varas rock glacier with that at La Quiaca during the same period of time, a temperature lapse rate of 7 °C km^{-1} can be established for the Cordillera Oriental. This allows us to calculate the 0 °C isotherm altitude. Accordingly to this relation, the 0 °C isotherm was situated at 5010 m a.s.l. during the 2011–2015 period. That is, ~500 m above the lower limit of the VARG and ~100 m above the highest peak of its rockwall source area. Moreover, the VARG is situated at elevations where the mean annual air temperature is 3.1 °C (5 year average; Table 2). This confirms the presence of mountain permafrost well below the 0 °C isotherm altitude. Air circulation on ventilated talus slopes has been reported as a possible mechanism responsible for permafrost occurrence under mean annual air temperature well above 0 °C in the Swiss Alps (e.g., chimney effect; [21]). In the case of the VARG, the high ground temperature at 5 and 50 cm depth (mean annual: 5.6 and 4.8 °C, respectively) would not support this idea, but deeper ground temperature records are needed to evaluate this mechanism. The occurrence of active rock glaciers in positive mean annual air temperature conditions has been reported in other sectors of the Central Andes ([75] and [4,10,15,76]).

On the other hand, according to the La Quiaca record, the air temperature rose by 0.8 °C in the last century, with a steep increase since 1991 (Fig. 7). A similar warming trend of ~0.1 °C/decade between 1939 and 1998 was established for the subtropical Andes [78]. In high-altitude mountains, a temperature increase results in the rise of the 0 °C isotherm altitude (or freezing level height), which can produce dramatic changes on the landscape and in water storage, such as permafrost [13,31]. The warming recorded by La Quiaca station represents 114 m upward movement of the 0 °C isotherm for the last century, in agreement with the tropical average rate of 10–20 m/decade calculated by Bradley et al. [12] for the last 30 years.

On the Varas rock glacier, small displacements registered by boulders 27 and 30 could be attributed to the internal ice degradation of the VIRG. Also, the inactivity of boulders 15 and 25, and probably the low displacement (5 cm/yr) of boulder 12 in the VARG are signs of its degradation. The air warming trend recorded in northwestern Argentina likely contributes to the rapid removal of the snow cover, increasing the albedo and exposing the Varas rock glacier to high solar radiation all year around. For the Andes of Santiago, Bodin et al. [10] demonstrated that the near-surface ground thermal regime at high altitudes is strongly influenced by the snow cover disappearance date. The lack of an insulation snow cover on the Varas rock glacier should produce an important ground warming with an increment of the active layer thickness and permafrost degradation.

High-altitude tropical ice-core records reveal that the present warming trend has no precedent for at least the last 2 ka [73]. Combining satellite image analysis and tree-ring records, Morales et al. [55] reconstructed lake area fluctuations over the 1407–2007 period in the neighboring southern Altiplano. Lake area exhibited a negative trend since the 1930s with an exceptional reduction over the entire period between 1976 and 2007. Arid conditions for the last century were also recorded in lake sediments of Pumacocha in the Peruvian Andes [8], denoting a similar regional pattern. These records indicate dry conditions during most of the last century with markedly increase during the last few decades. Thus, regional air temperature rise and precipitation decline during the last century should have a negative impact on the VARG activity.

We infer it is possible that the VARG is not totally adapted to, or in 'equilibrium' with, the present climatic conditions, given the regional high-altitude paleo-temperature record shows that the warming that occurred during the last ~100 yr is unprecedented in the context of the last 2 ka [73] and because rock glaciers can respond with a delay to climate changes (decades or longer; [32]). Also, this explains why active rock glaciers exist now in areas well below the 0 °C isotherm, as discussed above. Moreover, a decline of precipitation during the last century [55] should reduce the Varas rock glacier water input and the denudation rate of the mountain headwalls [4], consequently reducing the total amount of talus production and debris supply to the Varas rock glacier.

Signs of cryosphere degradation are also common elsewhere in the Central and tropical Andes. Pronounced glacier retreat during the last century has been widely documented (e.g., [39,60,69,73,78]). Frozen ground and permafrost degradation are more difficult to achieve since the ice is isolated through the surface from a thick-variable debris or ground layer, but some cases have been documented. For example, in the Morenas Coloradas active rock glacier, located at the Cordón del Plata (~33°S) of Argentina, Trombotto and Borzotta [74] detected an increase of the permafrost table depth on a rate between 15 and 25 cm/yr in the last decades due to climate warming. On the Chilean side of the Andes at similar latitudes, Monnier and Kinnard [53] documented the growth of a rock glacier derived from a debris-covered glacier. The debris-covered glacier transformation into a rock glacier is a consequence of less-favorable climatic conditions to exposed-ice preservation, from melting. The occurrence of surface downwasting and the growth of thermokarst depressions in debris-covered glaciers were reported in the Andes of central Chile (30–33°S) [10,54]. Based on geomorphic features and geoelectrical soundings, Francou et al. [27] detected signs of degradation on the Caquella active rock glacier (23°S) in the southern Bolivian Altiplano. The referred geomorphic features include depressions and a recently-open crevasse, which form a drainage line of meltwater in the lower part of the Caquella rock glacier. Geoelectrical soundings show low-ice concentration (30%) and even sectors with no ice evidence in the rock glacier interior.

Model simulations for the next century indicate the largest warming will occur in mountains ranges that extend high in the lower troposphere, predicting maximum temperature increase for the tropical and subtropical Andes [11]. This might raise the altitude of the 0 °C isotherm and reduce the mountain permafrost area, generating a negative impact on the cryosphere [12]. Under this scenario, many small glaciers are expected to disappear [19] and the permafrost arrested or reduced to the highest sector on the ranges. Rangecroft et al. [62] predicted that the 95% of the current permafrost area of Bolivia will shrink by the 2050s under the SRES A1B temperature scenario [52]. This situation may turn the VARG totally inactive. As glaciers and permafrost are important water reservoirs, the predicted warming may have negative consequences on communities of the tropical and subtropical Andes [13,18]. At the moment, it is unclear how present and future warm-

ing could impact the cryosphere of the arid Andes of northwestern Argentina, where many human settlements and diverse small-scale agriculture exists above 3000 m a.s.l., which are highly dependent on water resources for their subsistence. Future research should continue to focus on understanding the cryospheric response to climatic changes in this region.

5.4. Rock glacier formation since the deglaciation

Based on the characterization of movement (Figs. 3 and 4) and detailed geomorphology presented in this study, we propose the following sequence for the Varas rock glacier formation. The last glacial retraction in the area occurred after ~12 ka [49,82]. The lack of glacial depositional features in the host valley of the Varas rock glacier suggests that deglaciation was relatively fast (Fig. 2a and b). ~12 ka is a maximum age for the initial formation of the Varas rock glacier; this age may indeed seem to be quite old according to its geomorphological appearance (Fig. 2; [51]). Sometime after ~12 ka the VIRG formed, and at some time later it become inactive, and the VARG started developing. The time elapsed between the glacial retraction and the VIRG formation is unknown. The contrasting appearance between the VARG and the VIRG, and the fact that there are talus-derived rock glaciers where the former is partially overriding or cross cutting the latter (Fig. 2a), suggest that their formation corresponds to different climatic episodes instead of a continuum of change.

The relatively small size and the surface velocity of the VARG indicate a relative young age. To estimate the age (A) of the VARG we apply a simple equation ($A = l/v$; [4]) that relates its maximum longitude in the mean flow direction ($l = 312$ m) with the mean surface velocity ($v = 22.2$ cm/yr from 2012 to 2016 period). We obtain an age of ~1.4 ka for the VARG formation. Although this is a rough estimation, it is much younger than the maximum-limiting age, obtained for the regional deglaciation (~12 ka) in this area of the Cordillera Oriental. The incipient SAPL may have originated during the last centuries, based on its size, position and the high velocity recorded (~12 m/yr). Finally, during the last century, a regional warming trend could have led to the inactivity of the more-exposed sector of the VARG near boulders 15 and 25.

During the Holocene, several glacial advances and retreats have been documented in the Andes of Bolivia and Peru (e.g., [42,47,68,70]), which have not been recorded in the Andes of northwestern Argentina [49,81,82]. The lack of glacier evidence indicates that climate changes during the Holocene allowed glaciers to expand in the Bolivian and Peruvian Andes, but in northwestern Argentina the glacial equilibrium line altitude remained above the highest range altitude. We suggest that in northwestern Argentina climate changes such as cooling events during the Holocene generated rock glaciers instead of glacier expansions. Supportive this inference, only 27.5% of the rock glaciers of the Cordillera Oriental of Argentina are active [51]. For comparison, inactive (47.5%) and fossil (25%) forms prevail, implying that climate changes occurred recurrently after waning of the Late Pleistocene glaciations. These Holocene climatic changes resulted in the different types of rock glaciers superimposed on each other at present (e.g., Varas rock glacier). Furthermore, the lack of postglacial advances in the Cordillera Oriental allowed the preservation of hundreds of rock glaciers, which at present exhibit different activities, including fossil and inactive [51].

6. Conclusions

In the Cordillera Oriental of the subtropical arid Andes, geomorphic analyses, surface velocity measurements, and climate data allow us to infer present and past processes associated with the inactive and active Varas rock glacier. During four consecutive years, surface flow measurements on 30 boulders over the Varas rock glacier allowed us to corroborate the rock glacier activity classification previously made based on geomorphologic criteria. The active portion of the Varas rock glacier (VARG) has four boulders where no movement was registered. For the rest of the boulders, the displacement rates range between 40 and 125 cm/yr in the upper sector and between 5 and 24 cm/yr in the lower sector.

Mean annual air temperature for the 2011–2015 period on the VARG ranged between 2.6 and 3.3 °C, and altitude of the 0 °C isotherm was situated ~100 m above the highest peak of the VARG source area. Relatively high positive air and ground temperatures at the VARG produce the rapid removal of the snow, lowering its albedo and exposing the VARG to a great amount of energy from high incoming solar radiation. The warming trend recorded during the last century may be responsible for some signs of degradation on the Varas rock glacier. Specifically, the observed inactivity of two boulders (25 and 15) on lower elevations of the VARG, which are also located on an area relatively exposed to solar radiation. Given the steep warming trend recorded at La Quiaca station during the last two and half decades, and considering the comparison with regional paleoclimatic proxies, we infer it is possible that the VARG is not totally adapted to, or in 'equilibrium' with, the present climatic conditions.

Regarding past changes, after the definitive waning of the Pleistocene glaciation, we suggest that recurrent cooling stages, resulted in the different kinds of rock glaciers that are currently superimposed, such as the one we have focused in. This study contributes to the knowledge of behavior of the rock glaciers in the subtropical arid Andes, which are potential water recourses considered of vital importance in the context of Argentinean legislation.

Acknowledgments

We are grateful to the SECyT, FonCyT (PICT 2013-1371) and CONICET for the financial support of this research. We would like to thank Lucia Guerra, Pablo Heredia Barión, Brenda Alvarez and Francisco Muñoz for the assistance during the fieldwork and Eugenia Ferrero for providing the climate data of La Quiaca station. Special thanks to Fede Davila for differential GPS equipment. We also thank two anonymous reviewers for their useful comments that improved the manuscript. This is LDEO contribution # 8138.

Supplementary materials

Supplementary material associated with this article can be found, in the online version, at doi:10.1016/j.grj.2017.08.002.

References

[1] Ahumada AL. Periglacial phenomena in the high mountains of northwestern Argentina. South Afr J Sci 2002;98:166–70.
[2] Ahumada AL, Ibáñez Palacios GP, Toledo MA, Carilla J, Páez SV. El permafrost reptante, inventario y verificación en las cabeceras del río Bermejo. Geoacta 2014;39:123–37.
[3] Apaloo J, Brenning A, Bodin X. Interactions between seasonal snow cover, ground surface temperature and topography (Andes of Santiago, Chile, 33.5°S). Permafr Periglac Process 2012;23:277–91. doi:10.1002/ppp.1753.
[4] Azócar GF, Brenning A. Hydrological and geomorphological significance of rock glaciers in the dry Andes, Chile (27°–33°S). Permafr Periglac Process 2010;21:42–53. doi:10.1002/ppp.669.
[5] Barsch D. Rockglaciers: indicators for the present and former geoecology in high mountain environments berlin. Springer; 1996. p. 331.
[6] Baroni C, Carton A, Seppi R. Distribution and behaviour of rock glaciers in the Adamello-Presanella massif (Italian Alps). Permafr Periglac Process 2004;15:243–59. doi:10.1002/ppp.497.
[7] Bianchi AR, Yañez CE. Las precipitaciones en el noroeste argentino. INTA Estación Experimental Agropecuaria, Salta; 1992. p. 393.
[8] Bird BW, Abbott MB, Vuille M, Rodbell DT, Stansell ND, Rosenmeier MF. A 2,300-year-long annually resolved record of the South American summer monsoon from the Peruvian Andes. Proc Natl Acad Sci U S A 2011;108:8583–8. doi:10.1073/pnas.1003719108.

[9] Bodin, X, Francou, B, Arnaud, Y, Fabre, D, 2010. State and dynamics of a tropical rock glacier on the Altiplano (Bolivia, 21.5°S) during the last two decades. Ice and Climate Change: A View from the South, Valdivia, Chile, pp 62.

[10] Bodin X, Rojas F, Brenning A . Status and evolution of the cryosphere in the Andes of Santiago (Chile, 33.5°S.). Geomorphology 2010b;118:453–64. doi:10.1016/j.geomorph.2010.02.016.

[11] Bradley RS, Keimig FT, Diaz HF. Projected temperature changes along the American cordillera and the planned GCOS network. Geophys Res Lett 2004;31:2–5. doi:10.1029/2004GL020229.

[12] Bradley RS, Keimig FT, Diaz HF, Hardy DR. Recent changes in freezing level heights in the Tropics with implications for the deglacierization of high mountain regions. Geophys Res Lett 2009;36:1–4. doi:10.1029/2009GL037712.

[13] Bradley RS, Vuille M, Diaz HF, Vergara W. Threats to water supplies in the tropical Andes. Science 2006;312:1755–6. doi:10.1126/science.1128087.

[14] Brenning A. Geomorphological, hydrological and climatic significance of rock glaciers in the Andes of Central Chile (33–35°S). Permafr Periglac Process 2005;16:231–40. doi:10.1002/ppp.528.

[15] Brenning A. Climatic and geomorphological controls of rock glaciers in the Andes of Central Chile: combining statistical modelling and field mapping. Humboldt-Universität zu Berlin; 2005.

[16] Burger KC, Degenhardt JJ, Giardino JR. Engineering geomorphology of rock glaciers. Geomorphology 1999;31:93–132. doi:10.1016/S0169-555X(99)00074-4.

[17] Carrasco JF, Casassa G, Quintana J. Changes of the 0 °C isotherm and the equilibrium line altitude in central Chile during the last quarter of the 20th century. Hydrol Sci J 2005;50:933–48. doi:10.1623/hysj.2005.50.6.933.

[18] Chevallier P, Pouyaud B, Suarez W, Condom T. Climate change threats to environment in the tropical Andes: glaciers and water resources. Reg Environ Chang 2011;11:179–87. doi:10.1007/s10113-010-0177-6.

[19] Coudrain A, Francou B, Kundzewicz ZW. Glacier shrinkage in the Andes and consequences for water resources – Editorial. Hydrol Sci J 2005;50. doi:10.1623/hysj.2005.50.6.925.

[20] Croce FA, Milana JP. Internal structure and behaviour of a rock glacier in the arid Andes of Argentina. Permafr Periglac Process 2002;13:289–99. doi:10.1002/ppp.431.

[21] Delaloye R, Lambiel C. Evidence of winter ascending air circulation throughout talus slopes and rock glaciers situated in the lower belt of alpine discontinuous permafrost (Swiss Alps). Nor J Geogr 2005;59:194–203. doi:10.1080/00291950510020673.

[22] Esper Angillieri MY. A preliminary inventory of rock glaciers at 30°S latitude, Cordillera Frontal of San Juan, Argentina. Quat Int 2009;195:151–7. doi:10.1016/j.quaint.2008.06.001.

[23] DGA. Dinámica de glaciares rocosos en el chile semiárido: parte i plan de monitoreo. Chile: Ministerio De Obras Públicas, Dirección General De Aguas Unidad De Glaciología y Nieves; 2010 http://documentos.dga.cl/GLA5261ParteI.pdf.

[24] Diaz HF, Bradley RS, Ning L. Climatic changes in mountain regions of the american cordillera and the tropics: historical changes and future outlook. Arct, Antarct Alp Res 2014;46:735–43. doi:10.1657/1938-4246-46.4.735.

[25] Diaz HF, Graham NE. Recent changes in tropical freezing heights and the role of sea surface temperature. Nature 1996;383:152–5. doi:10.1038/383152a0.

[26] Falaschi D, Castro M, Masiokas M, Tadono T, Ahumada AL. Rock glacier inventory of the valles calchaquíes region (∼ 25°S), Salta, Argentina, derived from ALOS data. Permafr Periglac Process 2014;25:69–75. doi:10.1002/ppp.1801.

[27] Francou B, Fabre D, Pouyaud B, Jomelli V, Arnaud Y. Symptoms of degradation in a tropical rock glacier, Bolivian Andes. Permafr Periglac Process 1999;10:91–100.

[28] Garreaud RD, Vuille M, Compagnucci R, Marengo J. Present-day South American climate. Palaeogeogr Palaeoclimatol Palaeoecol 2009;281:180–95. doi:10.1016/j.palaeo.2007.10.032.

[29] González, MA, Tchilinguirian, P, Pereyra, F, Ramallo, E, Gonzalez, OE, 2004. Hoja Geológica 2366-IV Ciudad de Libertador General San Martín, provincias de Jujuy y Salta: SEGEMAR, scale 1:250.000, 1 sheet, 114 pp text.

[30] Haeberli W. Mountain permafrost - research frontiers and a special long-term challenge. Cold Reg Sci Technol 2013;96:71–6. doi:10.1016/j.coldregions.2013.02.004.

[31] Haeberli W, Gruber S. Global warming and mountain permafrost. In: Permafrost soils. Soil biology, vol. 16. Berlin: Springer; 2009. p. 205–18. doi:10.1007/978-3-540-69371-0_14.

[32] Haeberli W, Hallet B, Arenson L, Elconin R, Humlum O, Kääb A, et al. Permafrost creep and rock glacier dynamics. Permafr Periglac Process 2006;17:189–214. doi:10.1002/ppp.561.

[33] Harris SA, Pedersen DE. Thermal regimes beneath coarse blocky matherials. Permafr Periglac Process 1998;9:107–20.

[34] Hausmann H, Krainer K, Brückl E, Mostler W. Creep of two alpine rock glaciers-observation and modelling (Ötztal- and Stubai Alps, Austria). Grazer Schr Geogr Raumforsch 2007;43:145–50.

[35] Hirsch RM, Slack JR, Smith RA. Techniques of trend analysis for monthly water quality data. Water Resour 1982;20:107–21.

[36] Ikeda A, Matsuoka N. Pebbly versus bouldery rock glaciers: morphology, structure and processes. Geomorphology 2006;73:279–96. doi:10.1016/j.geomorph.2005.07.015.

[37] Ikeda A, Matsuoka N, Kääb A. A rapidly moving small rock glacier at the lower limit of the mountain permafrost belt in the Swiss Alps. In: Proceedings of the 8th international conference on permafrost, Zürich, Switzerland; 2003. p. 455–60.

[38] Ikeda A, Matsuoka N, Kääb A. Fast deformation of perennially frozen debris in a warm rock glacier in the Swiss alps: an effect of liquid water. J Geophys Res 2008;113:F01021. doi:10.1029/2007JF000859.

[39] IPCC Observations: cryosphere in: climate change 2013: the physical science basis Contribution of working group I to the fifth assessment report of the intergovernmental panel on climate change Observations: cryosphere in: climate change 2013: the physical science basis Contribution of working group I to the fifth assessment report of the intergovernmental panel on climate change. Stocker TF, Qin D, Plattner G-K, Tignor M, Allen SK, Boschung J, et al., editors. Cambridge, United Kingdom and New York, NY, USA: Cambridge University Press; 2013.

[40] Ishikawa M. Thermal regimes at the snow–ground interface and their implications for permafrost investigation. Geomorphology 2003;52:105–20. doi:10.1016/S0169-555X(02)00251-9.

[41] Janke JR, Bellisario AC, Ferrando FA. Classification of debris-covered glaciers and rock glaciers in the Andes of central Chile. Geomorphology 2015;241:98–121. doi:10.1016/j.geomorph.2015.03.034.

[42] Jomelli V, Favier V, Rabatel A, Brunstein D, Hoffmann G, Francou B. Fluctuations of glaciers in the tropical Andes over the last millennium and palaeoclimatic implications: a review. Palaeogeogr Palaeoclimatol Palaeoecol 2009;281:269–82. doi:10.1016/j.palaeo.2008.10.033.

[43] Kääb A, Frauenfelder R, Roer I. On the response of rockglacier creep to surface temperature increase. Glob Planet Change 2007;56:172–87. doi:10.1016/j.gloplacha.2006.07.005.

[44] Kendall M. Multivariate analysis. London: Charles Griffin y Company; 1975. p. 309.

[45] Krainer K, Mostler W. Flow velocities of active rock glaciers in the Austrian alps. Geogr Ann 2006;88(4):267–80.

[46] Lambiel C, Delaloye R. Contribution of real-time kinematic GPS in the study of creeping mountain permafrost: examples from the Western Swiss Alps. Permafr Periglac Process 2004;15:229–41. doi:10.1002/ppp.496.

[47] Licciardi JM, Schaefer JM, Taggart JR, Lund DC. Holocene glacier fluctuations in the Peruvian Andes indicate northern climate linkages. Science 2009;325:1677–9. doi:10.1126/science.1175010.

[48] Mann HB. Nonparametric tests against trend. Econometrica 1945;13:245–259.

[49] Martini MA, Kaplan MR, Strelin JA, Astini RA, Schaefer JM, Caffee MW, et al. Late Pleistocene glacial fluctuations in Cordillera Oriental, subtropical Andes. Quat Sci Rev 2017;171:245–59. doi:10.1016/j.quascirev.2017.06.033.

[50] Martini MA, Strelin JA, Astini RA. Distribución y caracterización de la geomorfología glaciar en la Cordillera Oriental de Argentina. Acta Geol Lilloana 2015;27:105–20.

[51] Martini MA, Strelin JA, Astini RA. Inventario y caracterización morfoclimática de los glaciares de roca en la Cordillera Oriental Argentina (entre 22° y 25° S). Rev Mex Ciencias Geol 2013;30:569–81.

[52] Mitchell TD, Osborn TJ. ClimGen: a flexible tool for generating monthly climate data sets and scenarios. Tyndall centre for climate change research working paper. Tyndall Centre for Climate Change; 2005 http://www.ccafs-climate.org/downloads/docs/Climgen-Downscaling-Tyndall.pdf.

[53] Monnier S, Kinnard C. Reconsidering the glacier to rock glacier transformation problem: new insights from the central Andes of Chile. Geomorphology 2015;238:47–55. doi:10.1016/j.geomorph.2015.02.025.

[54] Monnier S, Kinnard C, Surazakov A, Bossy W. Geomorphology, internal structure, and successive development of a glacier foreland in the semiarid Chilean Andes (Cerro Tapado, upper Elqui Valley, 30° 08′ S., 69° 55′ W.). Geomorphology 2014;207:126–40. doi:10.1016/j.geomorph.2013.10.031.

[55] Morales MS, Carilla J, Grau HR, Villalba R. Multi-century lake area changes in the Southern Altiplano: a tree-ring-based reconstruction. Clim Past 2015;11:1139–52. doi:10.5194/cp-11-1139-2015.

[56] Payne D. Climatic implications of rock glaciers in the arid Western Cordillera of the Central Andes. Glacial Geol Geomorphol 1998 1998, rp03/1998.

[57] Pepin N, Bradley RS, Diaz HF, Baraer M, Caceres EB, Forsythe N, et al. Elevation-dependent warming in mountain regions of the world. Nat Clim Chang 2015;5:424–30. doi:10.1038/nclimate2563.

[58] Perucca L, Esper Angillieri Y. A preliminary inventory of periglacial landforms in the Andes of La Rioja and San Juan, Argentina, at about 28°S. Quat Int 2008;190:171–9. doi:10.1016/j.quaint.2007.10.007.

[59] Perucca L, Angillieri MYE. Glaciers and rock glaciers' distribution at 28° SL, Dry Andes of Argentina, and some considerations about their hydrological significance. Environ Earth Sci 2011;64:2079–89. doi:10.1007/s12665-011-1030-z.

[60] Rabatel A, Francou B, Soruco A, Gomez J, Cáceres B, Ceballos JL, et al. Current state of glaciers in the tropical Andes: a multi-century perspective on glacier evolution and climate change. Cryosphere 2013;7:81–102. doi:10.5194/tc-7-81-2013.

[61] Rangecroft S, Harrison S, Anderson K, Magrath J, Castel AP, Pacheco P. A first rock glacier inventory for the Bolivian Andes. Permafr Periglac Process 2014;25:333–43. doi:10.1002/ppp.1816.

[62] Rangecroft S, Suggitt AJ, Anderson K, Harrison S. Future climate warming and changes to mountain permafrost in the Bolivian Andes. Clim Change 2016;137:231–43. doi:10.1007/s10584-016-1655-8.

[63] Rosenblüth B, Fuenzalida HA, Aceituno P. Recent temperature variations in southern South America. Int J Climatol 1997;17:67–85. doi:10.1002/(SICI)1097-0088(199701)17:1⟨67::AID-JOC120⟩3.0.CO;2-G.

[64] Salazar G, Checura Diaz MS, Denegri MJ, Tiba C. Identification of potential areas to achieve stable energy production using the SWERA database: a case study of northern Chile. Renew Energy 2015;77:208–16. doi:10.1016/j.renene.2014.11.094.
[65] Schrott L. Some geomorphological-hydrological aspects of rock glaciers in the Andes (San Juan, Argentina). Z Geomorphol Suppl 1996;104:161–73.
[66] Sen PK. Estimates of the regression coefficient based on Kendall's tau. J Am Stat Assoc 1968;63:1379–89.
[67] Serrano E, San José JJ, Agudo C. Rock glacier dynamics in a marginal periglacial high mountain environment: flow, movement (1991–2000) and structure of the Argualas rock glacier, the Pyrenees. Geomorphology 2006;74:285–96. doi:10.1016/j.geomorph.2005.08.014.
[68] Smith CA, Lowell TV, Owen LA, Caffee MW. Late Quaternary glacial chronology on Nevado Illimani, Bolivia, and the implications for paleoclimatic reconstructions across the Andes. Quat Res 2011;75:1–10. doi:10.1016/j.yqres.2010.07.001.
[69] Soruco A, Vincent C, Francou B, Gonzalez JF. Glacier decline between 1963 and 2006 in the Cordillera Real, Bolivia. Geophys Res Lett 2009;36:2–7. doi:10.1029/2008GL036238.
[70] Stansell ND, Rodbell DT, Licciardi JM, Sedlak CM, Schweinsberg AD, Huss EG, et al. Late glacial and Holocene glacier fluctuations at Nevado Huaguruncho in the Eastern Cordillera of the Peruvian Andes. Geology 2015;43:747–50. doi:10.1130/G36735.1.
[71] Taillant JD. Glaciers: the politics of ice. New York: Oxford University Press; 2015. p. 334.
[72] Taylor JR. An introduction to error analysis: the study of uncertainties in physical measurements. Sausalito, California: University Science Books; 1997. p. 327.
[73] Thompson L, Mosley-Thompson E, Brecher H, Davis M, Leo B, Les D, et al. Abrupt tropical climate change: past and present. Proc Natl Acad Sci 2006;103:10536–43.
[74] Trombotto D, Borzotta E. Indicators of present global warming through changes in active layer-thickness, estimation of thermal diffusivity and geomorphological observations in the Morenas Coloradas rockglacier, Central Andes of Mendoza, Argentina. Cold Reg Sci Technol 2009;55:321–30. doi:10.1016/j.coldregions.2008.08.009.
[75] Trombotto D, Buk E, Hernandez J. Monitoring of mountain permafrost in the central Andes, Cordon del Plata, Mendoza, Argentina. Permafr Periglac Process 1997;8:123–9. doi:10.1002/(SICI)1099-1530(199701)8:1⟨123::AID-PPP242⟩3.0.CO;2-M.
[76] Trombotto D, Buk E, Hernández J. Rockglaciers in the Southern Central Andes (approx. 33°–34°S), Cordillera Frontal, Mendoza, Argentina. Bamb Geogr, Schr 1999;19:145–73.
[77] Viviroli D, Archer DR, Buytaert W, Fowler HJ, Greenwood GB, Hamlet AF, et al. Climate change and mountain water resources: overview and recommendations for research, management and policy. Hydrol Earth Syst Sci 2011;15:471–504. doi:10.5194/hess-15-471-2011.
[78] Vuille M, Francou B, Wagnon P, Juen I, Kaser G, Mark BG, et al. Climate change and tropical Andean glaciers: past, present and future. Earth-Sci Rev 2008;89:79–96. doi:10.1016/j.earscirev.2008.04.002.
[79] Vuille M, Franquist E, Garreaud R, Lavado Casimiro WS, Cáceres B. Impact of the global warming hiatus on Andean temperature. J Geophys Res Atmos 2015;120:3745–57. doi:10.1002/2015JD023126.
[80] Wahrhaftig C, Cox A. Rock glaciers in the Alaska range. Geol Soc Am Bull 1959;70:383. doi:10.1130/0016-7606(1959)70[383:RGITAR]2.0.CO;2.
[81] Zech J, Terrizzano C, García-Morabito E, Veit H, Zech R. Timing and extent of late Pleistocene glaciation in the arid Central Andes of Argentina and Chile (22°–41°S). Cuad Investig Geogr 2017;43. In press. doi:http://doi.org/10.18172/cig.3235.
[82] Zech J, Zech R, Kubik PW, Veit H. Glacier and climate reconstruction at Tres Lagunas, NW Argentina, based on ^{10}Be surface exposure dating and lake sediment analyses. Palaeogeogr Palaeoclimatol Palaeoecol 2009;284:180–90. doi:10.1016/j.palaeo.2009.09.023.
[83] Zhou J, Lau KM. Does a monsoon climate exist over South America? J Clim 1998;11:1020–40. doi:10.1175/1520-0442(1998)011⟨1020:DAMCEO⟩2.0.CO;2.